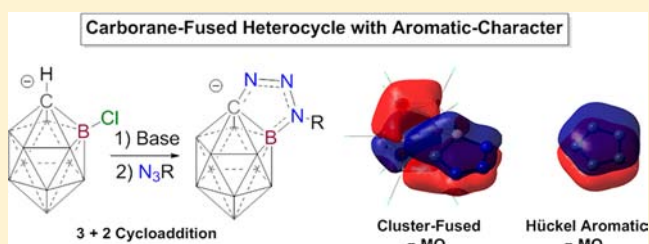


Click-Like Reactions with the Inert  $\text{HCB}_{11}\text{Cl}_{11}^-$  Anion Lead to Carborane-Fused Heterocycles with Unusual Aromatic CharacterJames H. Wright, II,<sup>†</sup> Christos E. Kefalidis,<sup>\*,‡</sup> Fook S. Tham,<sup>†</sup> Laurent Maron,<sup>‡</sup> and Vincent Lavallo<sup>\*,†</sup><sup>†</sup>Department of Chemistry, University of California Riverside, Riverside, California 92521, United States<sup>‡</sup>Department of Chemistry, CNRS & INSA, UPS, LPCNO, Université de Toulouse, 135 Avenue de Rangueil, F-31077, Toulouse France

## Supporting Information

**ABSTRACT:** The chlorinated carba-*closo*-dodecaborate anion  $\text{HCB}_{11}\text{Cl}_{11}^-$  is an exceptionally stable molecule and has previously been reported to be substitutionally inert at the B–Cl vertices. We present here the discovery of base induced cycloaddition reactions between this carborane anion and organic azides that leads to selective C and B functionalization of the cluster. A single crystal X-ray diffraction study reveals bond lengths in the heterocyclic portion of the ring that are shortened, which suggests electronic delocalization. Molecular orbital analysis of the ensuing heterocycles reveals that two of the bonding orbitals of these systems resemble two of the doubly occupied  $\pi$ -MOs of a simple 5-membered Hückel-aromatic, even though they are entangled in the carborane skeleton. Nucleus independent chemical shift analysis indicates that both the carborane cluster portion of the molecule and the carborane fused heterocyclic region display aromatic character. Computational methods indicate that the reaction likely follows a stepwise addition cyclization pathway.



## INTRODUCTION

Since their preparation and structural elucidation in the 1960s, icosahedral boron<sup>1</sup> and carborane<sup>2</sup> cluster compounds have captivated the imagination of the scientific community. With respect to the carboranes<sup>3</sup> and from an organic chemistry point of view, the hyper-coordinate carbon atoms seemingly defy the octet rule (Figure 1). The core of these clusters, which cannot

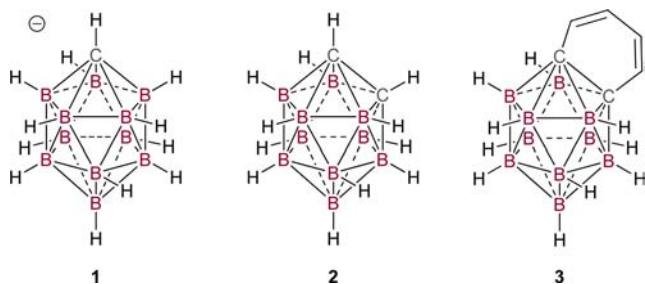


**Figure 1.** Isoelectronic and 3-D aromatic parent icosahedral carboranes  $\text{HCB}_{11}\text{H}_{11}^-$  **1**,  $\text{H}_2\text{C}_2\text{B}_{10}\text{H}_{10}$  **2**. Conjugation between the delocalized carborane skeletal electrons of **3** and its cluster fused 2-D  $\pi$ -system has been a matter of debate.

be described by classical 2-center-2-electron bonding models, feature a completely delocalized web of 26 skeletal electrons involved in 3-center-2-electron bonding between tangential p-type orbitals, as well as radial sp orbitals at the cluster vertices. Such polyhedra are said to possess 3-D aromaticity,<sup>4</sup> and analogies are often made to classical 2-D aromatic systems, such

as benzene. Indeed, similar to benzene, icosahedral carborane clusters display exceptional thermal stability, and the parent hydride derivatives **1** and **2** undergo reactions akin to electrophilic aromatic substitution at the B–H vertices.

A question that has long been asked is whether significant conjugation (or possibly aromaticity) can exist between a 3-D aromatic carborane and a fused 2-D  $\pi$ -ring system.<sup>5</sup> While  $\pi$ -donor–acceptor interactions are well documented for exocluster substituents of icosahedral carboranes,<sup>3,6</sup> extended conjugation or aromaticity is a matter of debate, as exemplified by the benzo-fused *ortho*-carborane **3**.<sup>5</sup> This molecule features localized C–C double bonds and also displays a carborane C–C bond length comparable to the parent carborane **2**.

Of the icosahedral carboranes the carba-*closo*-dodecaborate cluster  $\text{HCB}_{11}\text{H}_{11}^-$  **1**<sup>3b</sup> has historically received much less attention than its neutral and isoelectronic cousin *ortho*-carborane  $\text{H}_2\text{C}_2\text{B}_{10}\text{H}_{10}$  **2**.<sup>3a,7</sup> However, in the past 20 years or so there has been consistent growing interest in the use of this molecule and its derivatives for a variety of applications.<sup>3b</sup> The most familiar use of these molecules is as counter-anions for a variety of reactive cationic species.<sup>8</sup> The negative charge of these clusters is delocalized throughout the 12 cage atoms, resulting in a very weakly coordinating anion. This weak coordinative ability can be enhanced by halogenation of the cluster's boron vertices. Halogenation of the cage bestows these carborane anions with extraordinary inertness. As demonstrated

Received: March 29, 2013

Published: May 7, 2013

by Reed and co-workers,<sup>9</sup> polyhalogenated carborane anions are sufficiently unreactive that they resist decomposition even when paired with some of the most potent electron deficient species. Other groups have capitalized on these properties to generate very useful catalytic processes for the transition-metal-free activation and functionalization of persistent aliphatic fluorocarbons<sup>8h,i</sup> and fluoroaromatics,<sup>8g</sup> respectively. The anion of choice for most applications is the  $\text{HCB}_{11}\text{Cl}_{11}^-$  anion (**4**), which is particularly renowned for its weak coordinative abilities, ease of access,<sup>10</sup> and it is arguably the least reactive of the per-halogenated carba-*closo*-dodecaborates. Recently we reported a novel application of the carba-*closo*-dodecaborate anion core, namely, utilizing these species as super bulky, negatively charged, and weakly coordinating ligand R-groups.<sup>11</sup> Specifically, we demonstrated that a phosphine ligand bearing a  $\text{CB}_{11}\text{Cl}_{11}^-$  R-group, afforded anionic and zwitterionic single component gold catalysts that display the highest activity ever reported for the hydroamination of alkynes with primary aryl amines. This carborane ligand R-group is derived from the parent  $\text{HCB}_{11}\text{Cl}_{11}^-$  anion via deprotonation of the mildly acidic C–H vertex and subsequent reaction with an appropriate electrophile (Figure 2).

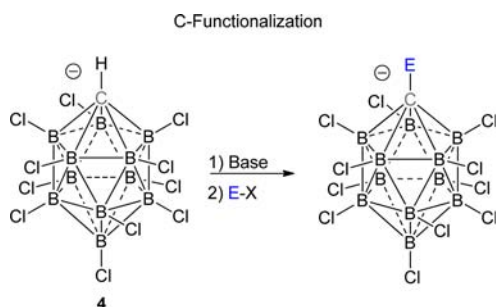


**Figure 2.** C-vertex of the perchlorinated carba-*closo*-dodecaborate anion ( $\text{HCB}_{11}\text{Cl}_{11}^-$ ) **4** can be deprotonated and functionalized with electrophiles. However, the B–Cl vertices are reportedly unreactive to any form of functionalization.

In contrast to the reactive C–H site, which allows for facile C-functionalization,<sup>3b,12</sup> the cluster B–Cl vertices of **4** are reported to be completely unreactive. In fact these B–Cl bonds are “supposedly” inert toward nucleophilic substitution, potent Brønsted bases, and oxidizing or reducing agents.<sup>13</sup> The inability to functionalize the B–Cl vertices of this cluster limits the molecular complexity that one can achieve when designing sophisticated building blocks for ligand design and other applications.

Here we report the discovery of a base-induced “click-like” cycloaddition reaction between the  $\text{HCB}_{11}\text{Cl}_{11}^-$  anion and organic azides that leads to selective C and B functionalization of the cluster. Further, evidence is presented that the ensuing heterocycles, which resemble 1,2,3-triazoles but with cluster fused C–B backbones, display aromatic characteristics.

## RESULTS AND DISCUSSION

**Synthesis and Characterization.** We reasoned that it might be possible to induce B–Cl substitution on the  $\text{HCB}_{11}\text{Cl}_{11}^-$  anion **4** by using the intramolecular advantage coupled with the formation of a delocalized, or possibly aromatic, system. Specifically, we envisioned the nucleophilic addition of the lithio-carborane **5** to a 1,3-dipole, such as an organic azide,<sup>14</sup> to generate a high energy dianionic

intermediate **6** that might be able to attack one of the adjacent boron atoms of the cluster (Figure 3). Because of the inherent

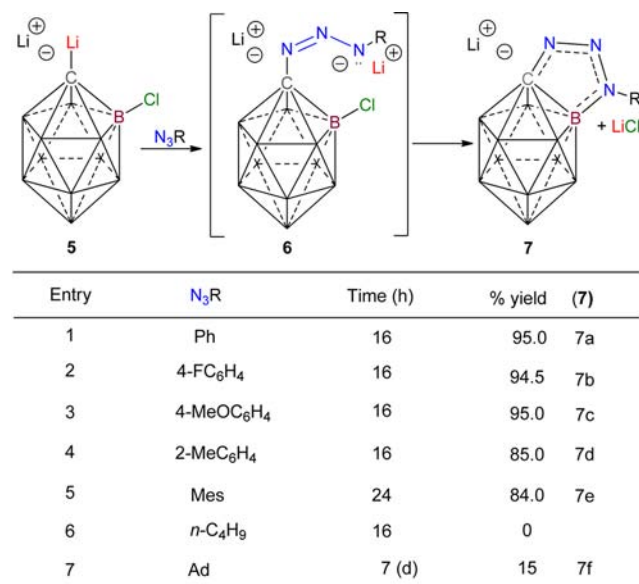


**Figure 3.** Lithio-carborane **5** undergoes cycloaddition reactions with organic azides that results in selective B–Cl functionalization, and produces the anionic heterocycles **7** (unlabeled icosahedron vertices = B–Cl).

anionic charge of the  $\text{CB}_{11}$  cluster core, heterocycles **7** might display enhanced exocluster delocalization, relative to neutral systems based on ortho-carborane **2**. Thus, carborane **4** was lithiated with *n*-BuLi to generate **5**, and subsequently treated with a fluorobenzene solution of phenyl azide ( $\text{N}_3\text{Ph}$ ). As indicated by <sup>11</sup>B Nuclear Magnetic Resonance (NMR) spectroscopy, no functionalization of the lithiated carborane **5** occurred at room temperature. However, upon heating the reaction mixture at 120 °C for 16 h, a new compound (**7a**) formed (Figure 3, entry 1). The <sup>11</sup>B spectrum of **7a** shows seven distinct resonances, indicating disruption of the pseudo  $C_{5v}$  symmetry in the cluster framework, suggesting B-substitution. Two-dimensional <sup>11</sup>B-<sup>11</sup>B correlation NMR spectroscopy confirmed that all seven resonances were interconnected in a single molecule. The natural abundance <sup>15</sup>N NMR spectra shows two resonances at 459 and 334 ppm, which are in the range (250–500 ppm, referenced to  $\text{NH}_3$ ) expected for a 2-D aromatic N-heterocycle.<sup>15</sup> We postulate that the third <sup>15</sup>N resonance is not observable because of the presence of a B–N linkage, which induces quadrupolar broadening of the signal. High Resolution Mass Spectrometry confirmed the identity of **7a**.

To explore the scope of the cycloaddition reaction, we next tested several electronically and sterically differentiated azide reaction partners. Aryl azides, featuring an electron donating *para*-methoxy or electron withdrawing *para*-fluoro substituent afforded the heterocycles **7b** and **7c** in excellent yields (Figure 3, entries 2 and 3). The reaction also tolerates sterically demanding mono- and diortho substituted aryl azides to form bulky heterocycles **7d** and **7e**, respectively (Figure 3, entries 4 and 5). Interestingly, when *n*-Butyl azide is used as an electrophile no heterocycle is formed (Figure 3, entry 6); instead clean C-alkylation occurs with liberation of  $\text{LiN}_3$ , affording the previously synthesized *n*-butylated carborane anion.<sup>12a</sup> In contrast when adamantyl azide is used, an

electrophile where backside attack is precluded, the heterocycle **7f** forms after extended heating as indicated by HRMS and  $^{11}\text{B}$  NMR (Figure 3, entry 8), but we have not yet devised a method to isolate it from organic impurities (presumably formed by thermal decomposition of  $\text{N}_3\text{Ad}$ ).

To investigate the molecular structure of these heterocycles a single crystal X-ray diffraction study was carried out on **7a** (cesium salt metathesis provided crystals of high quality). In the solid-state **7a** acts as a ligand, binding the cesium cation in an  $\eta^2$ -fashion, via N1 and N2 (Supporting Information, Figure S31). All 5 atoms of the heterocyclic portion of the molecule are coplanar (sum of internal pentagon angles =  $540^\circ$ ), and the nitrogen bearing the phenyl group (N3) is perfectly  $\text{sp}^2$  hybridized (sum of angles =  $360^\circ$ ), which suggests conjugation with the two other nitrogen atoms (Figure 4). Indeed, the N1–

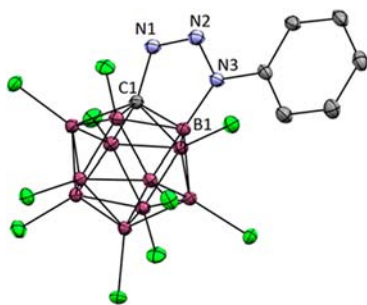


**Figure 4.** Solid-state structure of the anionic heterocycle **7a**. Counter-cation, solvent molecules, and hydrogen atoms omitted for clarity. Thermal ellipsoids drawn at the 50% probability level. Color coding (C-gray, N-blue, B-magenta, Cl-green).

N2(1.2823 (15) Å) and N2–N3(1.3538 (15) Å) bond lengths are significantly shorter than standard N–N single bonds (1.450 Å).<sup>16</sup> Although the exocyclic carbon–nitrogen distance (C1–N1 = 1.4460 (15) Å) is only slightly shorter than one would typically expect for a C–N single bond (1.454–1.485 Å),<sup>17</sup> the analogous N–B bond (B1–N3 = 1.4878 (16) Å) is short, which suggests multiple bond character (B–N single and double bond lengths 1.580 and 1.400 Å, respectively).<sup>18</sup> Interestingly, the C–B portion of the pentagon is dramatically shortened (C1–B1 = 1.6696 (18) Å) with respect to the other C–B linkages in the cluster (average C–B bond lengths = 1.7362 Å). Such a bond contraction is not observed with related neutral and diene-like benzocarboranes.<sup>5a</sup>

**Computational Study.** To gain further insight into the electronic structure of heterocycles **7** and probe the possibility of extended delocalization between the 2-D  $\pi$ -system of the heterocycle and the 3-D cluster framework, we performed various quantum chemical calculations, using **7a** as a model compound. The validity of the computational protocol used (B3PW91/6-31++G\*\*) was confirmed by the insignificant average absolute error in distances (<2%) and bond angles ( $\pm 0.2^\circ$ ), relative to the observed solid-state structure, allowing an accurate prediction of various geometrical, bonding, and electronic properties of **7a**. Close inspection of the molecular orbitals (MOs) of heterocycle **7a** reveals significant mixing between the carborane cage and the outer rings (5-member heterocycle and phenyl), indicating a strong interplay between the different systems. Of particular interest are three occupied  $\pi$ -type MOs (orbitals 96, 121, and 124). Two of these MOs (MOs 96 and 121, Figure 5(a)) contain areas of constructive

bonding that resemble two of the doubly occupied  $\pi$  MOs ( $\pi_1$  and  $\pi_2$ , Figure 5b) of a simple 5-membered Hückel-aromatic.

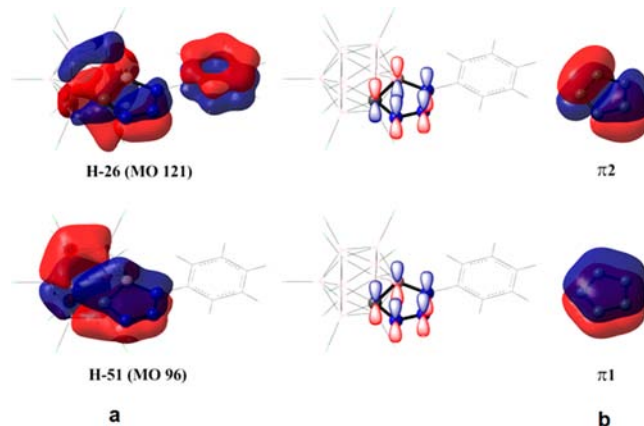


**Figure 5.** Molecular Orbitals. Bonding MOs (a) 96 and 121 of **7a** resemble two doubly occupied MOs ( $\pi_1$  and  $\pi_2$ ) (b) of a simple 5-membered ring aromatic. Chlorine orbital contributions omitted for clarity (For complete MOs, see Supporting Information, Figure S32).

However, these MOs differ in that the atomic p- $\pi$  orbitals of carbon and boron, which are used to complete the 5-membered ring  $\pi$ -bonding combinations, are at the same time strongly mixed with adjacent cluster orbitals to form extended delocalized MOs. The third  $\pi$ -bonding type MO, orbital 124, is delocalized over the entire molecule (Supporting Information, Figure S32). The highest occupied molecular orbital (HOMO) of the system has significant cluster orbital contributions, whereas the lowest unoccupied molecular orbital (LUMO) resides almost entirely outside of the 3-D framework (Supporting Information, Figure S32). The ultraviolet–visible spectrum displays a strong absorption band ( $\lambda_{\text{max}} = 313.0 \text{ nm}$ ), which corresponds to a HOMO–LUMO transition ( $\pi \rightarrow \pi^*$  excitation) and is supportive of extended delocalization between the cluster, heterocycle, and pendant benzene ring.

We next performed both an Atoms In Molecules (AIM)<sup>19</sup> and a Nucleus Independent Chemical Shift (NICS)<sup>20</sup> analysis. The AIM analysis confirms the presence of a ring critical point at the center of mass of the heterocycle and the carborane cage, which is supportive of delocalization of the 2-D  $\pi$ -system of the heterocycle, and the 3-D aromatic cluster respectively.<sup>21</sup> Values of magnetism based on Schleyer's NICS method indicate that the 5-membered heterocyclic portion of the molecule has appreciable aromatic character (NICS(0) =  $-7.8$ , NICS(1) =  $-8.8$ , and NICS(1)<sub>zz</sub> =  $-19.3$  ppm respectively). For comparison, benzene as the benchmark 2-D  $\pi$ -aromatic has a NICS(1)<sub>zz</sub> value of  $-29.2$  ppm. Likewise, NICS measurements (NICS(0) =  $-27.8$  ppm) taken at the center of the carborane region of the molecule indicate **7a** also retains its 3-D aromaticity ( $\text{HCB}_{11}\text{Cl}_{11}^-$  NICS(0) =  $-30.8$  ppm).

**Calculated Reaction Pathway.** Mechanistically, the formation of heterocycles **7** can be rationalized by either a stepwise addition cyclization pathway, as initially postulated, or a concerted reaction between the azide and a carbyryne-like intermediate<sup>22</sup> formed by the initial elimination of LiCl from the lithiocarborane. The latter pathway is ruled out since formation of such a C–B carbyryne is kinetically nonaccessible ( $\Delta E^\ddagger = 53.8 \text{ kcal.mol}^{-1}$ ) and thermodynamically unfavorable by  $52.5 \text{ kcal.mol}^{-1}$  (Figure 6).

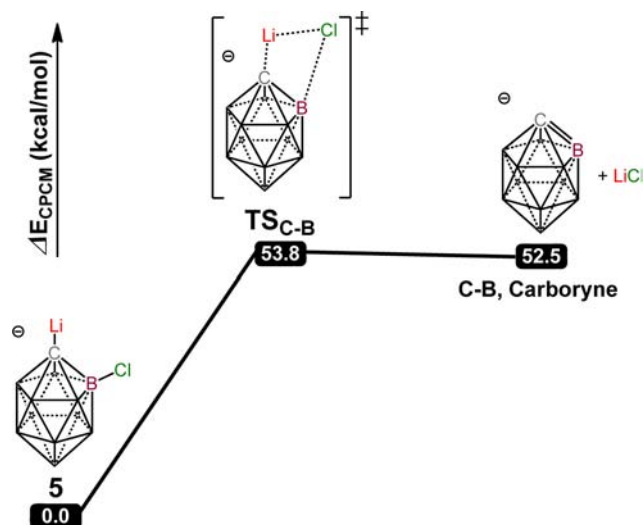


**Figure 6.** Calculated reaction pathway leading to C–B carborane. For clarity, most B–Cl linkages are not shown.

Hence, this unusual reaction likely follows a stepwise addition cyclization pathway (Figure 7). The C-nucleophilic

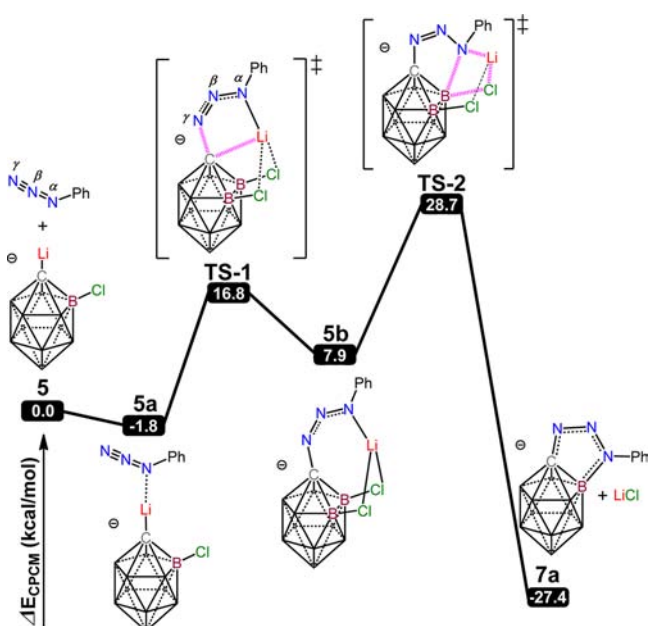


**Figure 7.** Calculated reaction pathway, leading to heterocycle 7a. For clarity, most B–Cl linkages are not shown.

lithiated carborane **5** first associates with the phenyl azide to form adduct **5a**. The formation of the latter is exothermic by only 1.8 kcal mol<sup>-1</sup>. Then electrophilic attack of the terminal N atom ( $\gamma$ -nitrogen) of the weakly coordinated phenyl azide to the nucleophilic carbon occurs, and leads to intermediate **5b** via a late transition state, **TS-1**. The C–Li bond length, in **TS-1**, is substantially increased with respect to **5a** (2.906 vs 2.048 Å). This relative long distance is the result of the interaction between the lithium atom and the two neighboring chlorides. At the same time, the distance between the  $\gamma$ -nitrogen of the azide and the carbon is significantly decreased by 2.33 Å, being 2.08 Å in **TS-1** and 4.41 Å in **5a**. In the vibrational mode corresponding to the imaginary frequency of **TS-1**, the dominant motions involve the stretching of Li atom toward

the carbon of the carborane, and the concomitant bending of the N<sub>3</sub> framework again toward the carbon of the carborane. The transformation of **5a** to **5b** requires a relative low energy barrier (18.6 kcal mol<sup>-1</sup>) and is endoergic (9.7 kcal mol<sup>-1</sup>). It should be noted that **TS-1** is indeed the true transition state that connects intermediates **5a** and **5b**, as it is the result of the IRC calculations. Moreover, based on natural population analysis, NPA, in **TS-1** the  $\gamma$ -nitrogen of the azide acquires an almost zero natural charge, the  $\beta$ -nitrogen a positive natural charge (0.116 lel), and the  $\alpha$ -nitrogen that is bonded to the phenyl group has a strong negative charge of –0.50 lel. This shows an allylic-like character of the azide and is the result of its coordination to the carborane. This allylic-like nature of the azide is even more pronounced in the intermediate **5b** (NPA's of  $\alpha$ -,  $\beta$ -, and  $\gamma$ -nitrogen, –0.51, 0.05, and –0.31 lel respectively). (For complete NPA charges, see Supporting Information, Figure S33)

The next step corresponds to the nucleophilic attack of  $\alpha$ -nitrogen to the typically inert B–Cl vertex of the cluster with simultaneous elimination of lithium chloride (**TS-2**). The activation barrier is needed for this process is 20.8 kcal mol<sup>-1</sup>. In the vibrational mode corresponding to the imaginary frequency of **TS-2**, the dominant motions involve the stretching of B–N(phenyl) bond, along with a simultaneous stretching of the B–Cl bond (leading to bond dissociation). It is worth noting that the forming N–B bond is 2.125 Å long, and the corresponding B–Cl linkage is elongated by 0.16 Å with respect to the intermediate **5b**. In addition, NPA analysis clearly shows the nature of the nucleophilic attack. Hence, in **TS-2** the  $\alpha$ -nitrogen of the azide acquires a strong negative charge of –0.49 lel and the boron a positive one (0.20 lel). More interestingly, the relative high activation barrier of this step is presumably due to the high accumulation of negative charges on each atom of the CN<sub>3</sub> framework increasing the electrostatic repulsion between carborane and the phenyl-azide (see Supporting Information, Figure S33); this step being the rate-determining in the reaction. This is in line with the experimental finding of a slow reaction, and the need for heat to achieve the cycloaddition. However, the high stability of the final product **7a** (–35.3 kcal mol<sup>-1</sup>), as well as the overall exothermicity of the reaction (–27.4 kcal mol<sup>-1</sup>), is the thermodynamic driving force for this process.

## CONCLUSION

The reactions outlined above demonstrate a viable strategy to functionalize the typically inert B–Cl vertices of the HCB<sub>11</sub>Cl<sub>11</sub><sup>–</sup> anion. Mechanistically, the reaction occurs via a novel stepwise addition cyclization pathway, that features a nucleophilic substitution reaction of a carborane B–Cl bond. This methodology allows access to structurally and electronically complex molecular fragments that have potential use as ligand building blocks, weakly coordinating anions, or components of advanced materials. Further, evidence presented in this study supports the notion that aromaticity can occur in two separate but fused 3-dimensional and 2-dimensional systems, such as an icosahedral carborane and a Hückel aromatic.

## EXPERIMENTAL SECTION

**General Considerations.** All manipulations were carried out using standard Schlenk or glovebox technique (O<sub>2</sub>, H<sub>2</sub>O < 1 ppm) under a dinitrogen or argon atmosphere. Solvents were dried on K or CaH<sub>2</sub>, distilled under argon, and passed through basic alumina before use.

Trimethyl ammonium undecachlorocborane and organic azides were prepared by literature methods.<sup>10,23</sup> All other reagents were purchased from commercial vendors and used without further purification. NMR spectra were recorded at room temperature on Bruker Avance 600 MHz, Varian Inova 400 MHz, or Varian Inova 300 MHz spectrometers. NMR chemical shifts are reported in parts per million (ppm). <sup>1</sup>H NMR and <sup>13</sup>C NMR chemical shifts were referenced to the NMR solvent peaks. <sup>11</sup>B NMR chemical shifts were externally referenced to BF<sub>3</sub>OEt<sub>2</sub>. Natural abundance <sup>15</sup>N NMR chemical shifts were externally referenced to NH<sub>3</sub>. The mass spectra were collected on an Agilent LCTOF Multimode-ESI/APCI with direct injection. The UV/vis spectra was obtained on a Varian Cary 50 UV/vis spectrophotometer.

**Quantum Chemical Calculations.** All density functional theory (DFT) calculations were carried out using the Gaussian09 program suite.<sup>24</sup> The entire gas-phase potential energy surface (PES) for the mechanism was computed at the B3PW91 level of theory,<sup>25,26</sup> while the 6-31G++(d,p) basis set was used for all atoms. To study the solvent effects, single point CPCM<sup>27</sup> calculations were conducted using fluorobenzene (dielectric constant,  $\epsilon = 5.42$ ) as solvent on the gas-phase optimized geometries of B3PW91, using the larger 6-311++G(2d,2p) basis set for all atoms. All energies given in the text are CPCM electronic energies. The nature of the species connected by a given transition state structure was confirmed by intrinsic reaction coordinate (IRC) calculations, while intrinsic reaction paths (IRPs)<sup>28</sup> were traced from the various transition structures to make sure that no further intermediates exist. Time-dependent density functional theory (TD-DFT)<sup>29–31</sup> calculations were performed on the equilibrium ground state geometries employing the same density functional and basis set used in geometry optimizations. The Davidson algorithm was used, in which the error tolerance in the square of the excitation energies and trial-vector orthonormality criterion were set to 10<sup>–8</sup> and 10<sup>–10</sup>, respectively. Analysis of the electron distribution function was made on the basis of QTAIM (quantum theory of atoms in molecules),<sup>19</sup> while the search and topological analysis of ring critical points (RCPs) were done using Multiwfn program.<sup>32</sup> Nucleus-Independent Chemical Shifts (NICS) values were computed at the same level of theory according to the procedure described by the Schleyer group.<sup>33</sup> The magnetic shielding tensor element was calculated for a ghost atom located at the center of the heterocycle ring (NICS(0)) and along the z-axis (NICS(1)<sub>zz</sub>).<sup>34</sup> It has been shown that the latter is a more reliable descriptor of aromaticity of a given system.<sup>35</sup> Negative (diatropic) NICS values indicate aromaticity, while positive (paratropic) values imply antiaromaticity. NMR shielding tensors were computed by the gauge-including atomic orbital method (GIAO),<sup>36–40</sup> as implemented in the GAUSSIAN09 series of programs using the same theoretical protocol used in geometry optimizations. The natural bond orbital (NBO) population analysis was performed using Weinhold's methodology.<sup>41,42</sup>

**Synthesis of Heterocycles 7.** *Li(THF)<sub>3</sub>[closo-PhN<sub>3</sub>-CB<sub>11</sub>Cl<sub>10</sub>] (7a).* HNMe<sub>3</sub>HCB<sub>11</sub>Cl<sub>11</sub> (2.00 g, 3.44 mmol) was dissolved in tetrahydrofuran (THF, 100 mL) in a Schlenk flask. Subsequent addition of *n*-butyllithium (2.89 mL, 7.22 mmol, 2.5 M in hexanes, over 15 min) afforded a white precipitate of the dilithio species, and the mixture was allowed to stir for 12 h. The suspension was then concentrated to 1.0 mL, then hexanes (200 mL) was added and the reaction stirred for 5 min. After allowing the precipitate to settle (15 min), the supernatant was removed via cannula filtration and discarded. The white powder was dried under high vacuum for 30 min and subsequently dissolved in fluorobenzene (40 mL). The solution was transferred to a thick walled high pressure Schlenk tube containing phenyl azide (879.4 mg, 7.383 mmol) and placed behind a blast shield where the reaction was heated for 16 h at 120 °C. After cooling the darkened reaction mixture to ambient temperature it was brought into a glovebox, and the precipitate was collected on a sintered glass filter. The solid was extracted with boiling fluorobenzene (3 × 100 mL) until only LiCl remained on the filter. The combined fluorobenzene fractions were concentrated to dryness, washed with hexane (3 × 20 mL), then diethyl ether (3 × 10 mL), and the off-white powder was collected on a clean sintered glass filter to afford pure 7a (2.7 g, 3.27 mmol, 95%

yield, mp 231 °C (dec.)). X-ray quality crystals of 7a(Cs<sup>+</sup>) were grown, after cesium salt metathesis in H<sub>2</sub>O, and subsequent dissolution of the precipitate in diethyl ether and layering with hexanes. HRMS: (Multimode-ESI/APCI) [M]<sup>–</sup>*m/z* calc'd for H<sub>3</sub>B<sub>11</sub>C<sub>7</sub>N<sub>3</sub>Cl<sub>10</sub> 603.8419, found: 603.8422. <sup>1</sup>H NMR(CDCl<sub>3</sub>, 300 MHz):  $\delta = 7.34$  (m, 1H), 7.47(m, 2H), 7.68(m, 2H); Note: <sup>1</sup>H NMR analysis indicates the lithium countercation of 7a retains three coordinated THF molecules.<sup>11</sup>B NMR (THF-d<sub>8</sub>, 192 MHz):  $\delta = -1.98, -8.98, -12.05, -12.65, -15.16, -15.88$ ; <sup>13</sup>C NMR (THF, 151 MHz):  $\delta = 141.46, 130.38, 126.98, 119.25, 85.31$  (C<sub>carborane</sub>); <sup>15</sup>N NMR (THF-d<sub>8</sub>, 61 MHz):  $\delta = 458.67, 333.55$ . UV:  $\lambda_{\text{max}} = 313.4$  nm (CH<sub>3</sub>CN).

*Li(THF)<sub>3</sub>[closo-4-FC<sub>6</sub>H<sub>4</sub>N<sub>3</sub>-CB<sub>11</sub>Cl<sub>10</sub>] (7b).* 7b was prepared in an analogous manner as 7a. HRMS: (Multimode-ESI/APCI) [M]<sup>–</sup>*m/z* calc'd for H<sub>4</sub>B<sub>11</sub>C<sub>7</sub>N<sub>3</sub>FC<sub>10</sub> 621.8325, found: 621.8351. <sup>1</sup>H NMR (CDCl<sub>3</sub>, 300 MHz):  $\delta = 7.14$  (m, 2H), 7.64 (m, 2H), Note: <sup>1</sup>H NMR analysis indicates the lithium countercation retains three coordinated THF molecules. <sup>11</sup>B NMR (CDCl<sub>3</sub>, 96 MHz):  $\delta = -5.38, -9.65, -13.06, -16.78$ ; <sup>13</sup>C NMR (CDCl<sub>3</sub>, 101 MHz):  $\delta = 161.53$  (d, <sup>1</sup>J(F, C) = 278 Hz), 136.05, 120.96 (d, <sup>3</sup>J(F, C) = 8.5 Hz), 116.94 (d, <sup>2</sup>J(F, C) = 23.0 Hz); Note: C<sub>carborane</sub> was not observed; <sup>19</sup>F NMR (CDCl<sub>3</sub>, 282 MHz):  $\delta = -114.9$  (tt, <sup>3</sup>J(H, F) = 8.4 Hz, <sup>4</sup>J(H, F) = 4.5 Hz); off-white powder with 94.6% yield.

*Li(THF)<sub>3</sub>[closo-4-MeOC<sub>6</sub>H<sub>4</sub>N<sub>3</sub>-CB<sub>11</sub>Cl<sub>10</sub>] (7c).* 7c was prepared in an analogous manner as 7a. HRMS: (Multimode-ESI/APCI) [M]<sup>–</sup>*m/z* calc'd for H<sub>7</sub>B<sub>11</sub>C<sub>8</sub>N<sub>3</sub>OCl<sub>10</sub> 633.8525, found: 635.8539. <sup>1</sup>H NMR (CDCl<sub>3</sub>, 300 MHz):  $\delta = 3.84$  (s, 3H), 6.97 (d, *J* = 9 Hz, 2H), 7.58 (d, *J* = 9 Hz, 2H), Note: <sup>1</sup>H NMR analysis indicates the lithium countercation retains three coordinated THF molecules. <sup>11</sup>B NMR (CDCl<sub>3</sub>, 96 MHz):  $\delta = -5.42, -9.82, -13.07, -17.02$ ; <sup>13</sup>C NMR (CDCl<sub>3</sub>, 101 MHz):  $\delta = 158.05, 133.68, 119.75, 114.71, 84.31$  (C<sub>carborane</sub>), 54.70; dark brown solid with 97.3% yield.

*Li(THF)<sub>3</sub>[closo-2-MeC<sub>6</sub>H<sub>4</sub>N<sub>3</sub>-CB<sub>11</sub>Cl<sub>10</sub>] (7d).* 7d was prepared in an analogous manner as 7a. HRMS: (Multimode-ESI/APCI) [M]<sup>–</sup>*m/z* calc'd for H<sub>7</sub>B<sub>11</sub>C<sub>8</sub>N<sub>3</sub>Cl<sub>10</sub> 617.8576, found: 617.8578. <sup>1</sup>H NMR (CDCl<sub>3</sub>, 300 MHz):  $\delta = 2.480$  (s, 3H), 7.32 (m, 3H), 7.67 (m, 1H) Note: <sup>1</sup>H NMR analysis indicates the lithium countercation retains three coordinated THF molecules. <sup>11</sup>B NMR (THF, 96 MHz):  $\delta = -6.59, -10.52, -13.43, -16.11, -17.37$ ; <sup>13</sup>C NMR (THF, 101 MHz):  $\delta = 141.78, 135.57, 130.53, 129.69, 127.64, 122.75, 87.09$  (C<sub>carborane</sub>), 23.05; dark brown solid with 82.0% yield.

*Li(THF)<sub>3</sub>[closo-MesitylN<sub>3</sub>-CB<sub>11</sub>Cl<sub>10</sub>] (7e).* 7e was prepared in an analogous manner as 7a. HRMS: (Multimode-ESI/APCI) [M]<sup>–</sup>*m/z* calc'd for H<sub>11</sub>B<sub>11</sub>C<sub>10</sub>N<sub>3</sub>Cl<sub>10</sub> 645.8890, found: 645.8909. <sup>1</sup>H NMR (CDCl<sub>3</sub>, 300 MHz):  $\delta = 2.30$  (s, 3H), 2.47 (s, 6H), 6.94 (s, 2H), Note: <sup>1</sup>H NMR analysis indicates the lithium countercation retains three coordinated THF molecules. <sup>11</sup>B NMR (CDCl<sub>3</sub>, 96 MHz):  $\delta = -2.50, -5.09, -10.17, -13.09, -17.50$ ; <sup>13</sup>C NMR (CDCl<sub>3</sub>, 101 MHz):  $\delta = 139.1, 135.5, 134.8, 131.1, 22.2, 20.8$ ; Note: C<sub>carborane</sub> was not observed. Dark brown oil with 84.2% yield.

*Li(THF)<sub>3</sub>[closo-AdamantylN<sub>3</sub>-CB<sub>11</sub>Cl<sub>10</sub>] (7f).* 7f was prepared in an analogous manner as 7a, except heating was continued for 1 week. HRMS: (Multimode-ESI/APCI) [M]<sup>–</sup>*m/z* calc'd for H<sub>4</sub>B<sub>11</sub>C<sub>7</sub>N<sub>3</sub>FC<sub>10</sub> 661.9193, found: 661.9204.

## ■ ASSOCIATED CONTENT

### 📄 Supporting Information

Experimental procedures, spectroscopic data, X-ray Crystallographic data and computations. This material is available free of charge via the Internet at <http://pubs.acs.org>.

## ■ AUTHOR INFORMATION

### Corresponding Author

\*E-mail: [vincent.lavallo@ucr.edu](mailto:vincent.lavallo@ucr.edu) (V.L.), [christos.kefalidis@insa-toulouse.fr](mailto:christos.kefalidis@insa-toulouse.fr) (C.E.K.).

## Author Contributions

The manuscript was written through contributions of all authors. All authors have given approval to the final version of the manuscript. These authors contributed equally.

## Notes

The authors declare no competing financial interest.

## ACKNOWLEDGMENTS

We are grateful to UCR and the ACS PRF (award # 52255-DNI3) for financial support of this work. L.M. is a member of the Institut Universitaire de France. ANR, CNRS, and UPS are acknowledged for financial support.

## REFERENCES

- (1) Pitochelli, A. R.; Hawthorne, F. M. *J. Am. Chem. Soc.* **1960**, *82*, 3228.
- (2) (a) Knoth, W. H. *J. Am. Chem. Soc.* **1967**, *89*, 1274. (b) Heying, T. L.; Ager, J. W.; Clark, S. L.; Mangold, D. J.; Goldstein, H. L.; Hillman, M.; Polak, R. J.; Szymanski, J. W. *Inorg. Chem.* **1963**, *2*, 1089. (c) Fein, M. M.; Bobinski, J.; Mayes, N.; Schwartz, N.; Cohen, M. S. *Inorg. Chem.* **1963**, *2*, 1111.
- (3) For reviews on the isoelectronic carborane clusters  $C_2B_{10}$  and  $CB_{11}^-$ , see refs 3a and 3b respectively. (a) Scholz, M.; Hey-Hawkins, E. *Chem. Rev.* **2011**, *111*, 7035. (b) Körbe, S.; Schreiber, P. J.; Michl, J. *Chem. Rev.* **2006**, *106*, 5208.
- (4) (a) Chen, Z.; King, R. B. *Chem. Rev.* **2005**, *105*, 3613. (b) King, R. B. *Chem. Rev.* **2001**, *101*, 1119.
- (5) (a) Copley, R. C. B.; Fox, M. A.; Gill, W. R.; Howard, J. A. K.; MacBride, J. A. H.; Peace, R. J.; Rivers, G. P.; Wade, K. *Chem. Commun.* **1996**, 2033. (b) Matteson, D. S.; Hota, N. K. *J. Am. Chem. Soc.* **1971**, *93*, 2893. (c) Hota, N. K.; Matteson, D. S. *J. Am. Chem. Soc.* **1968**, *90*, 3570. (d) Wu, S.-h.; Jones, M. *Inorg. Chem.* **1988**, *27*, 2005.
- (6) (a) Weber, L.; Kahlert, J.; Brockhinke, R.; Böbling, L.; Brockhinke, A.; Stammler, H.-G.; Neumann, B.; Harder, R. A.; Fox, M. A. *Chem.—Eur. J.* **2012**, *18*, 8347. (b) Dash, B. P.; Satapathy, R.; Gaillard, E. R.; Norton, K. M.; Maguire, J. A.; Chug, N.; Hosmane, N. S. *Inorg. Chem.* **2011**, *50*, 5485. (c) Fox, M.; Nervi, C.; Crivello, A.; Batsanov, A.; Howard, J. K.; Wade, K.; Low, P. J. *Solid State Electrochem.* **2009**, *13*, 1483. (d) Boyd, L. A.; Clegg, W.; Copley, R. C. B.; Davidson, M. G.; Fox, M. A.; Hibbert, T. G.; Howard, J. A. K.; Mackinnon, A.; Peace, R. J.; Wade, K. *Dalton Trans.* **2004**, 2786.
- (7) For recent examples of applications utilizing ortho-carborane, see 7a–c. (a) Spokoiny, A. M.; Machan, C. W.; Clingerman, D. J.; Rosen, M. S.; Wiester, M. J.; Kennedy, R. D.; Stern, C. L.; Sarjeant, A. A.; Mirkin, C. A. *Nat. Chem.* **2011**, *3*, 590. (b) Spokoiny, A. M.; Reuter, M. G.; Stern, C. L.; Ratner, M. A.; Seideman, T.; Mirkin, C. A. *J. Am. Chem. Soc.* **2009**, *131*, 9482. (c) Kusari, U.; Li, Y.; Bradley, M. G.; Sneddon, L. G. *J. Am. Chem. Soc.* **2004**, *126*, 8662.
- (8) (a) Kaleta, J.; Tarabek, J.; Akdag, A.; Pohl, R.; Michl, J. *Inorg. Chem.* **2012**, *51*, 10819. (b) Stoyanov, E. S.; Gunbas, G.; Hafezi, N.; Mascal, M.; Stoyanova, I. V.; Tham, F. S.; Reed, C. A. *J. Am. Chem. Soc.* **2012**, *134*, 707. (c) Volkis, V.; Douvris, C.; Michl, J. *J. Am. Chem. Soc.* **2011**, *133*, 7801. (d) Fete, M. G.; Havlas, Z. k.; Michl, J. *J. Am. Chem. Soc.* **2011**, *133*, 4123. (e) Tsurumaki, E.; Hayashi, S.-Y.; Tham, F. S.; Reed, C. A.; Osuka, A. *J. Am. Chem. Soc.* **2011**, *133*, 11956. (f) Stoyanov, E. S.; Stoyanova, I. V.; Reed, C. A. *J. Am. Chem. Soc.* **2011**, *133*, 8452. (g) Allemann, O.; Duttwyler, S.; Romanato, P.; Baldrige, K. K.; Siegel, J. S. *Science* **2011**, *332*, 574. (h) Douvris, C.; Nagaraja, C. M.; Chen, C.-H.; Foxman, B. M.; Ozerov, O. V. *J. Am. Chem. Soc.* **2010**, *132*, 4946. (i) Stoyanov, E. S.; Stoyanova, I. V.; Tham, F. S.; Reed, C. A. *J. Am. Chem. Soc.* **2010**, *132*, 4062. (j) Valášek, M.; Štursa, J.; Pohl, R.; Michl, J. *Inorg. Chem.* **2010**, *49*, 10247. (k) Stoyanov, E. S.; Stoyanova, I. V.; Tham, F. S.; Reed, C. A. *J. Am. Chem. Soc.* **2009**, *131*, 17540. (l) Douvris, C.; Ozerov, O. V. *Science* **2008**, *321*, 1188. (m) Stoyanov, E. S.; Stoyanova, I. V.; Tham, F. S.; Reed, C. A. *J. Am. Chem. Soc.* **2008**, *130*, 12128. (n) Molinos, E.; Brayshaw, S. K.; Kociok-Köhn, G.; Weller, A. S. *Organometallics* **2007**, *26*, 2370. (o) Molinos, E.; Brayshaw, S. K.; Kociok-Köhn, G.; Weller, A. S. *Dalton Trans.* **2007**, 4829. (p) Douglas, T. M.; Molinos, E.; Brayshaw, S. K.; Weller, A. S. *Organometallics* **2007**, *26*, 463. (q) Clarke, A. J.; Ingleson, M. J.; Kociok-Koehn, G.; Mahon, M. F.; Patmore, N. J.; Rourke, J. P.; Ruggiero, G. D.; Weller, A. S. *J. Am. Chem. Soc.* **2004**, *126*, 1503.
- (9) Reed, C. A. *Acc. Chem. Res.* **2009**, *43*, 121.
- (10) Gu, W.; McCulloch, B. J.; Reibenspies, J. H.; Ozerov, O. V. *Chem. Commun.* **2010**, 46, 2820.
- (11) Lavallo, V.; Wright, J. H., II; Tham, F. S.; Quinlivan, S. *Angew. Chem., Int. Ed.* **2013**, *52*, 3172.
- (12) (a) Ramirez-Contreras, R.; Ozerov, O. V. *Dalton Trans.* **2012**, *41*, 7842. (b) Himmelspach, A.; Sprenger, J. A. P.; Warneke, J.; Zähres, M.; Finze, M. *Organometallics* **2011**, *31*, 1566. (c) Finze, M.; Sprenger, J. A. P.; Schaack, B. B. *Dalton Trans.* **2010**, 39, 2708.
- (13) Boéré, R. T.; Bolli, C.; Finze, M.; Himmelspach, A.; Knapp, C.; Roemmele, T. L. *Chem.—Eur. J.* **2013**, *19*, 1784.
- (14) For an example of a cycloaddition reaction of an organic azide with a boron cluster, see: Küpper, S.; Carroll, P. J.; Sneddon, L. G. *J. Am. Chem. Soc.* **1992**, *114*, 4914.
- (15) Witanowski, M. *Nitrogen NMR*; Witanowski, M., Webb, G. A., Eds.; Plenum Press: London, U.K., 1973; pp 163.
- (16) *CRC Handbook of Chemistry and Physics*, 92nd ed.; CRC Press: Boca Raton, FL, 2011.
- (17) Allen, F. H.; Kennard, O.; Watson, D. G.; Brammer, L.; Orpen, A. G.; Taylor, R. *J. Chem. Soc., Perkin Trans. 2* **1987**, S1.
- (18) Bosdet, M. J. D.; Piers, W. E. *Can. J. Chem.* **2009**, *87*, 8.
- (19) Bader, R. F. W. *Atoms in Molecules: A Quantum Theory*; Oxford University Press: New York, 1990.
- (20) Chen, Z. F.; Wannere, C. S.; Corminboeuf, C.; Puchta, R.; Schleyer, P. v. R. *Chem. Rev.* **2005**, *105*, 3842.
- (21) Poater, J.; Duran, M.; Solà, M.; Silvi, B. *Chem. Rev.* **2005**, *105*, 3911.
- (22) (a) Ren, S.; Qiu, Z.; Xie, Z. *J. Am. Chem. Soc.* **2012**, *134*, 3242. (b) Wang, S. R.; Qiu, Z.; Xie, Z. *J. Am. Chem. Soc.* **2011**, *133*, 5760. (c) Qiu, Z.; Ren, S.; Xie, Z. *Acc. Chem. Res.* **2011**, *44*, 299. (d) Wang, S. R.; Qiu, Z.; Xie, Z. *J. Am. Chem. Soc.* **2010**, *132*, 9988.
- (23) Spencer, L. P.; Altwer, R.; Wei, P.; Gelmini, L.; Gauld, J.; Stephan, D. W. *Organometallics* **2003**, *22*, 3841.
- (24) Frisch, M. J.; Trucks, G. W.; Schlegel, H. B.; Scuseria, G. E.; Robb, M. A.; Cheeseman, J. R.; Scalmani, G.; Barone, V.; Mennucci, B.; Petersson, G. A.; Nakatsuji, H.; Caricato, M.; Li, X.; Hratchian, H. P.; Izmaylov, A. F.; Bloino, J.; Zheng, G.; Sonnenberg, J. L.; Hada, M.; Ehara, M.; Toyota, K.; Fukuda, R.; Hasegawa, J.; Ishida, M.; Nakajima, T.; Honda, Y.; Kitao, O.; Nakai, H.; Vreven, T.; Montgomery, Jr., J. A.; Peralta, J. E.; Ogliaro, F.; Bearpark, M.; Heyd, J. J.; Brothers, E.; Kudin, K. N.; Staroverov, V. N.; Kobayashi, R.; Normand, J.; Raghavachari, K.; Rendell, A.; Burant, J. C.; Iyengar, S. S.; Tomasi, J.; Cossi, M.; Rega, N.; Millam, J. M.; Klene, M.; Knox, J. E.; Cross, J. B.; Bakken, J.; Adamo, C.; Jaramillo, J.; Gomperts, R.; Stratmann, R. E.; Yazyev, O.; Austin, A. J.; Cammi, R.; Pomelli, C.; Ochterski, J. W.; Martin, R. L.; Morokuma, K.; Zakrzewski, V. G.; Voth, G. A.; Salvador, P.; Dannenberg, J. J.; Dapprich, S.; Daniels, A. D.; Farkas, Ö.; Foresman, J. B.; Ortiz, J. V.; Cioslowski, J.; Fox, D. J. *Gaussian 09, Revision A.02*; Gaussian, Inc.: Wallingford, CT, 2009.
- (25) Becke, A. D. *J. Chem. Phys.* **1993**, *98*, 5648.
- (26) Perdew, J. P.; Wang, Y. *Phys. Rev. B* **1992**, *45*, 13244.
- (27) (a) Barone, V.; Cossi, M. *J. Phys. Chem. A* **1998**, *102*, 1995. (b) Cossi, M.; Rega, N.; Scalmani, G.; Barone, V. *J. Comput. Chem.* **2003**, *24*, 669.
- (28) (a) Gonzalez, C.; Schlegel, H. B. *J. Chem. Phys.* **1989**, *90*, 2154. (b) Gonzalez, C.; Schlegel, H. B. *J. Phys. Chem.* **1990**, *94*, 5523.
- (29) Gisbergen, S. J. A.; Kootstra, F.; Schipper, P. R. T.; Gritsenko, O. V.; Snijders, J. G.; Baerends, E. J. *J. Phys. Rev. A* **1998**, *57*, 1556.
- (30) Jamorski, C.; Casida, M. E.; Salahub, D. R. *J. Chem. Phys.* **1996**, *104*, 5134.
- (31) Bauernschmitt, R.; Ahlrichs, R. *Chem. Phys. Lett.* **1996**, *256*, 454.
- (32) Lu, T.; Chen, F. *J. Comput. Chem.* **2012**, *33*, 580.

- (33) Schleyer, P. v. R.; Maerker, C.; Dransfeld, A.; Jiao, H.; Hommes, N. J. R. v. R. *J. Am. Chem. Soc.* **1996**, *118*, 6317.
- (34) Fallah-Bagher-Shaidei, H.; Wannere, C. S.; Corminboeuf, C.; Puchta, R.; Schleyer, P. v. R. *Org. Lett.* **2006**, *8*, 863.
- (35) Stanger, A. *J. Org. Chem.* **2006**, *71*, 883.
- (36) London, F. *J. Phys. Radium* **1937**, *8*, 397.
- (37) McWeeny, R. *Phys. Rev.* **1962**, *126*, 1028.
- (38) Ditchfield, R. *Mol. Phys.* **1974**, *27*, 789.
- (39) Wolinski, K.; Hinton, J. F.; Pulay, P. *J. Am. Chem. Soc.* **1990**, *112*, 8251.
- (40) Cheeseman, J. R.; Trucks, G. W.; Keith, T. A.; Frisch, M. J. *J. Chem. Phys.* **1996**, *104*, 5497.
- (41) Reed, A. E.; Agtiss, L. A.; Weinhold, F. *Chem. Rev.* **1988**, *88*, 899.
- (42) Weinhold, F. In *The Encyclopedia of Computational Chemistry*; Schleyer, P. v. R., Ed.; John Wiley & Sons: Chichester, U.K., 1998; p 1792.